# Spiral Terraces and Spin Frustration in Layered Antiferromagnetic Cr (001) Films

T. Kawagoe,[1] Y. Iguchi,[2] T. Miyamachi,[2] A. Yamasaki,[2] and S. Suga[2]

[1]*Division of Natural Science, Osaka Kyoiku University, Osaka 582-8582, Japan*
[2]*Graduate School of Engineering Science, Osaka University, Osaka 560-8531, Japan*
(Received 10 June 2005; published 9 November 2005)

We have successfully fabricated a novel type of high-density spiral terraces on Cr(001) films. The influence of nanoscale spiral terraces on layered antiferromagnetic ordering of Cr(001) films has been studied at room temperature by direct imaging of both topographic and magnetic structures using spin-polarized scanning tunneling spectroscopy. Spin frustration and asymmetric magnetic ordering due to dense spiral terraces are observed. Sizable modification of the layered antiferromagnetic order is found to be originating from the topological asymmetry as confirmed by the continuum micromagnetic simulation.

Magnetic structures of submicron lateral sizes of ferromagnetic films have been widely studied in the past [1]. For future developments of spin-electronic devices as well as fundamental physics of magnetism, a general understanding of the interplay between high-density nanoscale structures and magnetic properties is important. While exchange coupling between the ferromagnetic-antiferromagnetic interface is applied to the spin-electronic devices [2], little is known about the magnetic domain structure of antiferromagnetic (AF) films. Since there is no magnetostatic energy due to the stray field in AF materials, the origin of the magnetic domain structure is generally unclear in contrast to the cases of ferromagnets.

Here we focus on a Cr(001) surface that exhibits a layered (topological) AF order. The layered AF order of the surface is now a well-known subject where its magnetism is strongly correlated with the surface topography as theoretically introduced [3], and experimentally verified [4,5]. Therefore the Cr(001) surface is an ideal system to study the interplay between nanoscale structure and magnetism. The interest originates from the microscopic defects, such as steps and screw dislocations, which modify the AF order by spin frustration. Magnetically sensitive imaging techniques with nanometer spatial resolution, such as spin-polarized scanning tunneling microscopy and spectroscopy (SP-STM/STS) [6], is essential to study these phenomena. Only a few investigations focusing on spin frustrations of AF order have been so far reported [5,7,8].

In this Letter, we present a successful fabrication of high-density nanoscale AF spiral terraces and direct imaging of spin frustrated magnetic structures of Cr(001) surface by SP-STM/STS. It should be noted that the present work handles a novel type of Cr(001) films in contrast to the previous works which were focused on the influence of steps and screw dislocations upon the magnetic structure of the surface [7]. Spin frustration and characteristic magnetic ordering due to adjacent spiral terraces are observed for the first time, which can be explained by the micromagnetic simulation.

The experiments were performed in a UHV system consisting of molecular-beam epitaxy growth and STM chambers. The base pressure of both chambers was better than $5 \times 10^{-11}$ Torr. The details of our apparatus were described elsewhere [9]. A 100-nm-thick Au (001) seed layer was epitaxially grown at $250\,°C$ on a 3 nm Cr-precovered MgO(001) substrate. 9-nm-thick Cr films were then deposited on the clean Au(001) by electron beam evaporation with a growth rate of $0.3\,nm/min$. The pressure during the Cr evaporation was better than $2 \times 10^{-10}$ Torr. The two step growth technique [9] was employed for the growth of Cr layers on Au(001).

All STM experiments were performed at room temperature (RT) in a constant-current mode. Spatially resolved maps of the differential conductivity ($dI/dV$), together with topographic images, were obtained by using a lock-in technique. We used 2-nm-thick Fe-coated $W$ tips, which were sensitive to the in-plane magnetic moments [6].

Figure 1(a) shows a topographic STM image of the Cr(001) film (9 nm in thickness). In contrast to the flat terraces with islands for 4-nm-thick Cr films [9], 9-nm-thick Cr layers form steps and spiral terraces. The key factors for the successful fabrication of dense spiral Cr terraces on Au(001) may be (i) the large size of atomically flat terraces of the Au(001) surface and (ii) the proper
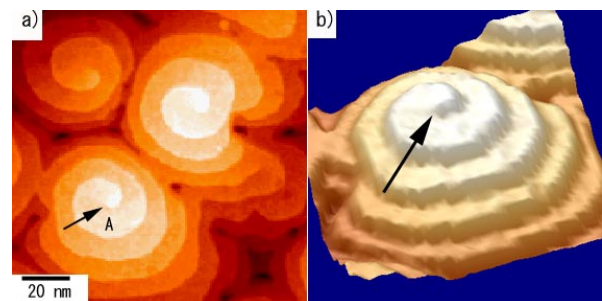


FIG. 1 (color online). (a) STM topographic image of 9-nm-thick Cr(001) film. (b) Zoom into one spiral pattern [named A in (a)] in a three-dimensional mode. A screw dislocation is indicated by the end of the black arrow.

growth rate and thickness of the Cr film. The use of a 3-nm-thick Cr buffer layer might have been essential for the large flat Au(001) surface. Three spiral patterns are visible in Fig. 1(a). The typical width of the spiral terraces is 15 nm. The height of the steps separating neighboring terraces corresponds always to the monatomic layer height. Figure 1(b) shows one of the spiral structures [named A in Fig. 1(a)] in a three-dimensional view, where the geometric structure is more clearly seen. At the center of each spiral pattern, a screw dislocation is clearly visible as indicated by an arrow. All of the spiral patterns originate from screw dislocations. One can see different chirality of screw dislocations in Fig. 1(a).

The spiral patterns have been observed in a large number of crystals [10] and are interesting from the viewpoint of crystal growth [11]. Layered AF order was observed on the Cr(001) stepped surface with ferromagnetic coupling in a single atomic terrace and AF coupling between adjacent terraces separated by a monatomic step [5,7,9]. The presence of spiral terraces with monatomic steps in layered AF order of Cr(001), therefore, induces a spin frustration.

The averaged $dI/dV$ spectrum of the Cr(001) film shows a distinct peak at $-50$ mV, which corresponds to the spin-polarized surface state [12]. The $dI/dV$ signal intensity for spin-dependent tunneling can be described by

$$dI/dV \propto (1 + P_t P_s \cos\theta), \qquad (1)$$

where $P_t$ and $P_s$ are the spin polarization of the tip and the sample, respectively [6]. $\theta$ is the mutual angle between the tip and the sample magnetization. Since the tip magnetization is fixed and $P_s$ is considered to be constant, we could image the surface magnetic structure with respect to the tip magnetization when the sample bias voltage ($V_s$) is tuned to a certain value near the Cr(001) surface state peak position [5,9].

Figs. 2(a) and 2(b) show large scale STM images of the topography (a), and the corresponding $dI/dV$ magnetic signal (b) of the Cr(001) film obtained simultaneously from the same area at $V_s = -100$ mV. The topographic feature is almost equivalent to that in Fig. 1(a) and many spiral terraces separated by monatomic steps are recognized. We have observed distinct magnetic contrast [13] in Fig. 2(b). By careful comparison of the two images of Figs. 2(a) and 2(b), one recognizes that the $dI/dV$ magnetic signal intensity level alternates when the monatomic height of terraces is crossed away from the spiral terraces. This is consistent with the layered AF order, which was already observed for the bulk Cr(001) surfaces [5] as well as for Cr(001) films [14].

The layered AF order is still maintained even on most spiral terraces. Figure 3(a) shows a zoomed magnetic $dI/dV$ image into the two spiral patterns indicated in the left bottom black box in Fig. 2(b). The two spiral patterns show the same chirality and the distance between the two screw dislocations is 75 nm. Figure 3(b) shows the $dI/dV$
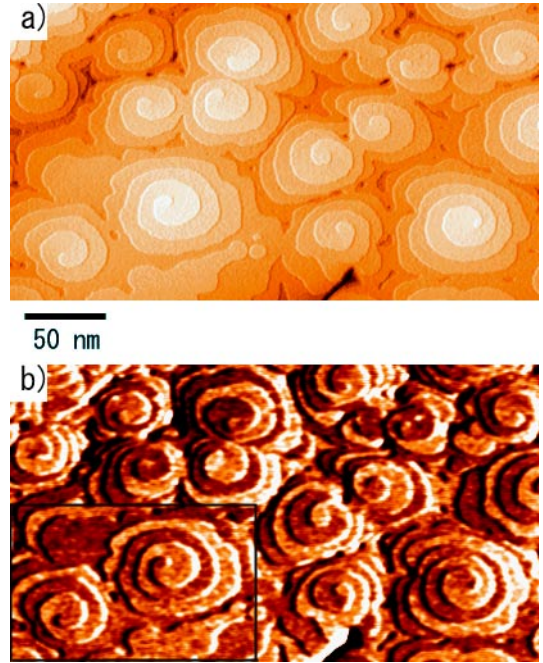


FIG. 2 (color online).   STM images of (a) the topography and (b) $dI/dV$ magnetic signal obtained simultaneously from the same area of a 9-nm-thick Cr(001) film with use of an Fe-coated $W$ tip ($V_s = -100$ mV).

magnetic signal along the white curved arrow on a spiral terrace. The observed magnetic contrast changes gradually along the white curved arrow with saturation below 40 and above 140 nm. Although the Fe-coated $W$ tip is usually sensitive to the in-plane magnetic component of the sample, a small out-of-plane magnetic component cannot be excluded. Therefore we cannot distinguish between the Néel or Bloch type walls unless a different tip with out-of-plane sensitivity is used. In our analysis, however, we assumed the in-plane magnetization component [7]. This $dI/dV$ profile $f(x)$ is well described with the standard 180°-domain wall profile [1],

$$f(x) = \alpha\left\{\tanh\left(\frac{x - x_0}{w}\right)\right\} + \beta, \qquad (2)$$

where $2w$ corresponds to the domain wall width and $\alpha$ and $\beta$ are related to the spin-dependent and spin-independent $dI/dV$ signal, respectively [7]. The best fitted parameters of $2w = 86 \pm 6$ nm, $\alpha = 0.073 \pm 0.002$, and $\beta = 1.36 \pm 0.01$ were derived from Fig. 3(b).

This gradual change of the magnetic contrast indicates that the magnetization rotates continuously around the center of the spiral terrace like a ferromagnetic vortex structure [15]. This origin is certainly a spin frustration due to spiral terraces. In contrast to the ferromagnetic vortex structure, the spin frustration of the AF order in the present case compensates only by 180° rotation of the magnetization. The maximum magnetic contrast corresponds to the layered AF order and a deviation from the
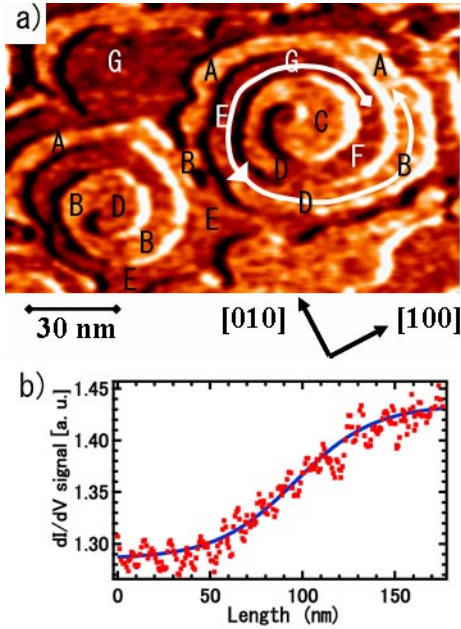
FIG. 3 (color online). (a) Zoomed $dI/dV$ magnetic image of
the black box indicated in Fig. 2(b) with use of an Fe-coated $W$
tip ($V_s = -100$ mV). The positions from A to G correspond to
the region names in Table I. (b) The $dI/dV$ magnetic signal
along the white curved arrow in Fig. 3(a) ($V_s = -100$ mV). The
solid curve represents a fit by Eq. (2).



FIG. 4 (color online). (a) Zoomed $dI/dV$ magnetic image of
the black box indicated in Fig. 2(b). The arrows indicate the
magnetization directions estimated according to Eq. (1) and
Table I. (b) The magnetic structure simulated to (a). The
directions of the magnetizations are represented by the arrows.

maximum magnetic contrast can be recognized as the spin
frustration. We notice in Fig. 2(b) that such frustrations are
induced in the region near the screw dislocations and
between two spirals as shown later more clearly in
Fig. 4(a).

The magnetic structure was deduced from the observed
$dI/dV$ magnetic signal intensity by assuming the orienta-
tion of the tip magnetization and the constant magnitude of
the Cr moments. Here we assume that the tip magnetiza-
tion is parallel to the bcc [100] direction, which is one of
the principal axes of layered AF order [16]. In order to
derive the magnetization direction, the $dI/dV$ signals are
averaged in many pixels and the deviation angle $\theta$ from the
[100] direction is evaluated as shown in Table I for the
positions from A to G in Fig. 3(a) with the proper choice of
the sign of $\theta$ to realize monotonous spin rotation. The
derived magnetic structure is schematically shown in
Fig. 4(a) by arrows. Obviously, the observed magnetic
structure on spiral terraces is rather complicated compared
with a ferromagnetic vortex structure and asymmetric to
the straight line connecting the two screw dislocations.

In the case of the layered AF ordered surface like
Cr(001), the spin frustration occurs when the screw dis-
location exists. Indeed, Kleiber *et al.* observed the spin
frustration induced by two screw dislocations on the bulk
Cr(001) surface [5]. Namely, a 180° domain wall connects
the two screw dislocations by a straight line, where the
frustrated regions are spread out isotropically [7], in con-

trast to our observed features. Although the mechanism of
the spin frustration on the present spiral terraces resembles
that by two screw dislocations on the bulk Cr(001) surface,
there exists a clear difference between the two cases. The
topological effects of spiral terraces are thought to be
responsible for the observed magnetic contrast.

In order to understand its origin, we have calculated the
magnetic structure of these adjacent spiral terraces with
micromagnetic simulations. Since the lateral size of the
spiral patterns is in the submicron range, the observed
magnetic structure can be treated within a continuum
micromagnetic theory. The simulations were performed
by using the micromagnetic simulation program OOMMF
[17]. The shape and the lateral size of the simulated model
are taken as the same as the observed STM image, allowing

TABLE I. Evaluation of the deviation angle $\theta$ of magnetiza-
tion from the [100] direction.

| Region name | $dI/dV$ [arb. units] | $\theta$ (°) |
|---|---|---|
| A | $1.44 \pm 0.01$ | 0 |
| B | $1.42 \pm 0.01$ | $\pm 41$ |
| C | $1.39 \pm 0.01$ | $\pm 68$ |
| D | $1.36 \pm 0.01$ | $\pm 90$ |
| E | $1.33 \pm 0.01$ | $\pm 112$ |
| F | $1.31 \pm 0.01$ | $\pm 128$ |
| G | $1.28 \pm 0.01$ | $\pm 180$ |

P H Y S I C A L   R E V I E W   L E T T E R S

direct comparison between the observed and calculated magnetic structures. The lateral size shown in Fig. 4(b) is 155 nm × 90 nm. The mesh cell was set to $0.288 \times 0.288 \times 2$ nm$^3$. Since spin frustrations are expected, we give a negative exchange interaction at the step edge and a positive exchange in the single atomic terrace, corresponding to the layered AF nature of the Cr(001) surface. The energy terms consist of exchange and anisotropy energies. It is not necessary to take into account the demagnetization term owing to the no-stray field in the layered AF Cr(001) surface. The equilibrium magnetic configuration is derived by minimizing the total energy as a function of the orientation of the magnetization under the constraint of constant magnetization. We used the following material parameters of Cr as the exchange stiffness $A_{ex} = 1 \times 10^{-11}$ J/m, the magnetocrystalline anisotropy $K_u = 1.77 \times 10^3$ J/m$^3$, and the surface exchange coefficient of AF interaction $\delta = -2 \times 10^{-3}$ J/m$^2$. The values of $A_{ex}$ and $K_u$ are the same as Ref. [7], and $\delta$ is the same as the layered coupling constant between Fe and Cr [18]. The uniaxial anisotropy direction is parallel to the [100] direction.

The result of simulation is shown in Fig. 4(b). The red (blue) or gray (dark) and white contrasts represent that the magnetization is parallel (antiparallel) and perpendicular to the [100] direction, respectively. The layered AF order appears in a series of adjacent terraces as well as in the most part of spiral terraces. The frustrated regions [white regions in Fig. 4(b)] are evident near the center of each spiral and in the lower part of the right spiral. The observed magnetic structure is clearly asymmetric with respect to the straight line connecting two screw dislocations. If one compares Fig. 4(a) and 4(b), one recognizes a qualitative agreement of the magnetizations in the frustrated regions. We have also observed and simulated another two adjacent spiral terraces with the same chirality, which is opposite to that in Fig. 4(a). The simulated spin alignments are also in good qualitative agreement with the observed result. Thus the spin arrangements on the spiral terraces are well understood by the micromagnetic simulations which take into account the exchange and anisotropy energy terms.

In conclusion, the first direct imaging of the magnetic structure of high-density spiral terraces on Cr(001) was successfully obtained at RT by spin-polarized STS. The asymmetric behavior of the spin frustration observed on and between spiral terraces with AF order is well explained by micromagnetic simulation. These findings are clearly different from the previous works focused on the influence of low density screw dislocations.

[1] A. Hubert and R. Schäfer, *Magnetic Domains* (Springer-Verlag, Berlin, 1998).

[2] A. E. Berkowitz and K. Takano, J. Magn. Magn. Mater. **200**, 552 (1999).

[3] S. Blügel, D. Pescia, and P. H. Dederichs, Phys. Rev. B **39**, 1392 (1989).

[4] R. Wiesendanger, H. J. Güntherodt, G. Güntherodt, R. J. Gambino, and R. Ruf, Phys. Rev. Lett. **65**, 247 (1990).

[5] M. Kleiber, M. Bode, R. Ravlić, and R. Wiesendanger, Phys. Rev. Lett. **85**, 4606 (2000).

[6] M. Bode, Rep. Prog. Phys. **66**, 523 (2003).

[7] R. Ravlić, M. Bode, A. Kubetzka, and R. Wiesendanger, Phys. Rev. B **67**, 174411 (2003).

[8] U. Schlickum, N. Janke-Gilman, W. Wulfhekel, and J. Kirchner, Phys. Rev. Lett. **92**, 107203 (2004).

[9] T. Kawagoe, Y. Iguchi, A. Yamasaki, Y. Suzuki, K. Koike, and S. Suga, Phys. Rev. B **71**, 014427 (2005).

[10] C. Kittel, *Introduction to Solid State Physics* (John Wiley & Sons, New York, 1976), 5th ed.

[11] W. K. Burton, N. Cabrera, and F. C. Frank, Phil. Trans. R. Soc. A **243**, 299 (1951).

[12] J. A. Strocio, D. T. Pierce, A. Davies, R. J. Celotta, and M. Weinert, Phys. Rev. Lett. **75**, 2960 (1995).

[13] Large contrasts are observed near the step edges in Fig. 2(b), which depend on the scan directions, due to the change of the tunneling current across the monatomic step. These contrasts are therefore not magnetic, but artificial origins induced by conventional STM operation.

[14] T. Kawagoe, Y. Suzuki, M. Bode, and K. Koike, J. Appl. Phys. **93**, 6575 (2003).

[15] T. Shinjo, T. Okuno, R. Hassdrof, K. Shigeto, and T. Ono, Science **289**, 930 (2000).

[16] E. Fawcett, Rev. Mod. Phys. **60**, 209 (1988).

[17] The Object Oriented Micromagnetic Framework (OOMMF) Project at NIST (http://math.nist.gov/oommf/). We used the OOMMF program, Version 1.2a3.

[18] D. T. Pierce, J. Unguris, R. J. Celotta, and M. D. Stiles, J. Magn. Magn. Mater. **200**, 290 (1999).